

Article

Synthesis of New RE³⁺ Doped Li_{1+x}Ta_{1-x}Ti_xO₃ (RE: Eu, Sm, Er, Tm, and Dy) Phosphors with Various Emission Colors

Hiromi Nakano ^{1*}, Shiho Suehiro ¹, Shohei Furuya ¹, Hiroyuki Hayashi ² and Shinobu Fujihara ³

¹ Toyohashi University of Technology, Tempaku, Toyohashi 441-8580, Japan; E-Mails: s113517@edu.tut.ac.jp (S.S.); s123440@edu.tut.ac.jp (S.F.)

² KRI, Inc., Chudoji Minami-machi, Shimogyo-ku, Kyoto 600-8813, Japan; E-Mail: h-hayasi@kri-inc.jp

³ Keio University, Yokohama 223-8522, Japan; E-Mail: shinobu@aplc.keio.ac.jp

* Author to whom correspondence should be addressed; E-Mail: hiromi@crfc.tut.ac.jp; Tel.: +81-532-44-6606; Fax: +81-532-44-6610.

Received: 19 April 2013; in revised form: 5 May 2013 / Accepted: 8 June 2013 /

Published: 11 July 2013

Abstract: New phosphors with various emission colors for RE³⁺ doped Li_{1+x}Ta_{1-x}Ti_xO₃ (LTT) (RE: Eu, Sm, Er, Tm, and Dy) were synthesized by electric furnace at 1423 K for 15 h. The microstructure of the host material and the photoluminescence (PL) property were determined and compared to those of RE³⁺ doped Li_{1+x}Nb_{1-x}Ti_xO₃ (LNT). In the LTT phosphor, the highest PL intensity was achieved for the mixture composition Li_{1.11}Ta_{0.89}Ti_{0.11}O₃ with a LiTaO₃ structure, although it has an M-phase superstructure. In the LTT host material, the effective activators were Eu³⁺ and Sm³⁺ ions, in contrast to the LNT host material. Here, we discuss the relationship between PL property and the host material's structure.

Keywords: solid solution; host material; phosphor; structure; photoluminescence

1. Introduction

In the ternary Li₂O-M₂O₅-TiO₂ system, Li_{1+x-y}M_{1-x-3y}Ti_{x+4y}O₃ (M: Nb or Ta, 0.06 ≤ x ≤ 0.33, 0 ≤ y ≤ 0.17) forms with a superstructure, and this is known as the M-phase. Since the discovery of the M-phase for Li_{1+x-y}Nb_{1-x-3y}Ti_{x+4y}O₃ (LNT) by Castrejon *et al.* [1,2], such structures have been investigated [3–6]. The M-phase superstructure is formed by periodical insertion of an intergrowth

layer in the matrix having a trigonal structure. The relationship between dielectric property and period of the intergrowth layer of the M-phase has been studied [7,8]. To apply this unique structure to the host material of a phosphor, new phosphors have been investigated based on LNT synthesized by a conventional electric furnace [9,10]. A homogeneous material was, however, synthesized at 1373 K for 24 h. We have succeeded in synthesizing an LNT solid solution having a superstructure by millimeter-wave heating for only 1 h above 1173 K [11]. The technique has also been applied to the synthesis of rare-earth doped LNT phosphor [12,13]. The photoluminescence (PL) intensity of LNT:Eu³⁺ at 625 nm was much higher than that of LiNbO₃:Eu.[12] Rare-earth-doped LiTaO₃ (RE³⁺: Pr³⁺ [14], Er³⁺ [15], Tb³⁺ [16] Eu³⁺ [17] and Tm³⁺ [18]) have also been reported by other groups. Recently, we have reported a new red phosphor based on the quaternary Li_{1+x}(Ta_{1-z}Nb_z)_{1-x}Ti_xO₃ (LTNT, 0.05 ≤ x ≤ 0.25, 0 ≤ z ≤ 0.625) solid solution as a host material. The PL intensity of the LTNT:Eu³⁺ phosphor was found to be dependent on the concentration of Eu³⁺, Ti⁴⁺, Nb⁵⁺, and Ta⁵⁺ ions [19].

In this work, rare-earth doped Li_{1+x}Ta_{1-x}Ti_xO₃ (LTT) phosphors with various emission colors were synthesized by an electric furnace and compared to LNT phosphors for annealing condition, host material's structure, and PL property.

2. Results and Discussion

As we reported previously for the Li_{1+x-y}Nb_{1-x-3y}Ti_{x+4y}O₃ (LNT, 0 ≤ x ≤ 0.25, y = 0) system [12], the PL intensity was clearly improved by the addition of TiO₂, which could affect the coordination state of the Eu³⁺ ion and/or induce a structural distortion around this ion. The most important factor is thus expected to be the TiO₂ content in the Li_{1+x}Ta_{1-x}Ti_xO₃ (LTT) solid solution. The optimal TiO₂ concentration was then determined at the maximum emission peak upon excitation at around 399 nm. Red emission of the Eu³⁺-doped LTT was observed at an excitation wavelength of 399 nm due to the intraconfigurational ⁷F₀-⁵L₆ transition. The maximum emission peak at around 624 nm is associated with the hypersensitive electric-dipole ⁵D₀-⁷F₂ transition in the Eu³⁺ ion. Figure 1 shows the relationships among the PL intensity, internal quantum efficiency, and the TiO₂ content in the ternary Li-Ta-Ti-O system upon varying the TiO₂ content from x = 0 to 0.25 at a fixed Eu₂O₃ concentration of 2.5 wt %. The highest PL intensity is found for the composition of Li_{1.11}Ta_{0.89}Ti_{0.11}O₃ (x = 0.11, y = 0), where the chemical composition is based on the mixture ratio. The internal quantum efficiency revealed a high value of 84.8%, but the highest value appeared in Li_{1.18}Ta_{0.82}Ti_{0.18}O₃ with x = 0.18. The discrepancy in the x values that give the highest PL intensity and the highest quantum efficiency may come from the different measurement apparatus. Because the integrating sphere was used in the internal quantum efficiency measurement, the "x = 0.18" value is supposed to be more appropriate to discuss the relationship between the host crystal composition and the emission properties. The incorporation of Eu³⁺ ions in the crystal structure of LTT would cause the overlapping of orbitals with the adjacent anions, resulting in efficient red-light emission due to the hypersensitive ⁵D₀-⁷F₂ transition in Eu³⁺.

The LNT phosphor with composition of Li_{1.11}Nb_{0.89}Ti_{0.11}O₃: x = 0.11 was also found to have the highest PL intensity [9]. Here, the host material's structure was compared between LNT and LTT. In Li_{1.11}Nb_{0.89}Ti_{0.11}O₃, the superstructure is formed by periodical insertion of the intergrowth layer with 14.3 nm spacing into a matrix with a trigonal structure (Figure 2b), and satellite reflections appeared around the (012) in the XRD pattern (Figure 2a). The superstructure was formed by doping of the Ti⁴⁺

ion, and the period was controlled by the Ti content, as described in our previous paper [11]. On the other hand, $\text{Li}_{1.11}\text{Ta}_{0.89}\text{Ti}_{0.11}\text{O}_3$ has no superstructure but only a basic structure of LiTaO_3 (Figure 2c). The results revealed that the composition area of the M-phase with a superstructure is different between LNT and LTT. In our recent paper [20], the refined structure was compared between LiTaO_3 and $\text{Li}_{1.11}\text{Ta}_{0.89}\text{Ti}_{0.11}\text{O}_3$ by the Rietveld method from powder X-ray diffraction data. The composition was determined as $\text{Li}(\text{Ta}_{0.89}\text{Ti}_{0.11})\text{O}_{2.945}$ from the final structure model, in which the Ti ion is located at the Ta site. By doping of the Ti^{4+} ion into LiTaO_3 , the $\langle\text{Li-O}\rangle$ distance of the (LiO_{12}) polyhedron in the LiTaO_3 structure ($R3c$) changed from 0.274 nm to 0.270 nm, and the $[(\text{Ta,Ti})\text{O}_6]$ octahedra are all comparable with each other. As a result, the structure is stable without a superstructure.

Figure 1. Relationships among PL intensity, internal quantum efficiency, and TiO_2 content in $\text{Li}_{1+x}\text{Ta}_{1-x}\text{Ti}_x\text{O}_3$ host material.

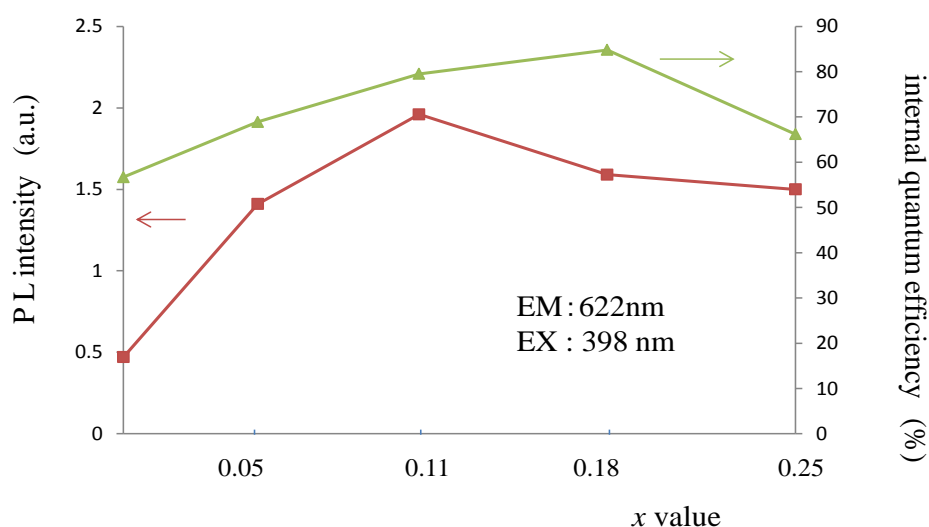
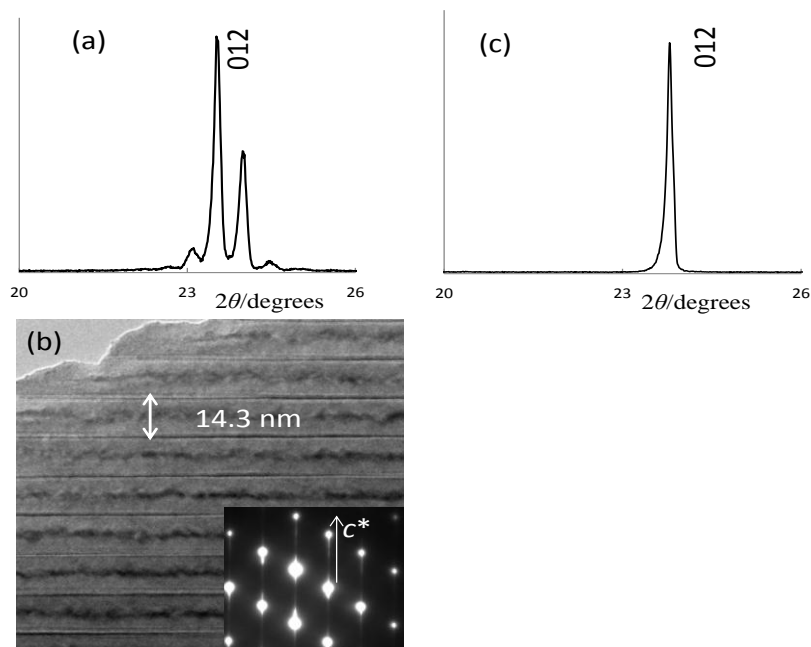


Figure 2. Structures of $\text{Li}_{1.11}\text{M}_{0.89}\text{Ti}_{0.11}\text{O}_3$ (M: Nb or Ta) host material: (a–b) LNT; and (c) LTT.



In Eu^{3+} -doped LNT phosphor, an annealing time of 24 h is preferable to that of 10 h because the superstructure forms during long-time annealing [10]. In the previous work, PL intensity might have been related to the structural distortion due to the superstructure. Indeed, PL intensity increased with increasing sintering time. In the LTT, the relationship between the annealing time and PL intensity should be clear. Figure 3 shows this relationship in $\text{Li}_{1.11}\text{Ta}_{0.89}\text{Ti}_{0.11}\text{O}_3:\text{Eu}^{3+}$ phosphor. The results show that the best annealing time is 15 h. For shorter annealing time, a small amount of EuTaO_4 was detected around 30 degrees in Figure 4. To diffuse the Eu^{3+} ion into the LiTaO_3 structure homogeneously as an activator, the annealing time needs to be 15 h. We confirmed that the Eu^{3+} ion is randomly distributed over the Li site because the electron-density peak at the Li/Eu site of Eu-doped LTT was higher than that at the Li site of LTT [20]. The composition determined by the Rietveld method was $(\text{Li}_{0.977}\text{Eu}_{0.023})(\text{Ta}_{0.89}\text{Ti}_{0.11})\text{O}_{2.968}$, which has a small amount of oxygen vacancies. The crystal structure of LiTaO_3 is flexible with respect to the substitutions of Eu for Li and Ti for Ta, in which the $\langle\text{Li-O}\rangle$ distance of the (LiO_{12}) polyhedron is 0.270 nm and 0.272 nm in $\text{Li}(\text{Ta}_{0.89}\text{Ti}_{0.11})\text{O}_{2.945}$ and $(\text{Li}_{0.977}\text{Eu}_{0.023})(\text{Ta}_{0.89}\text{Ti}_{0.11})\text{O}_{2.968}$, respectively.

Figure 3. Relationship between PL intensity and annealing time in $\text{Li}_{1.11}\text{Ta}_{0.89}\text{Ti}_{0.11}\text{O}_3:\text{Eu}^{3+}$ phosphor.

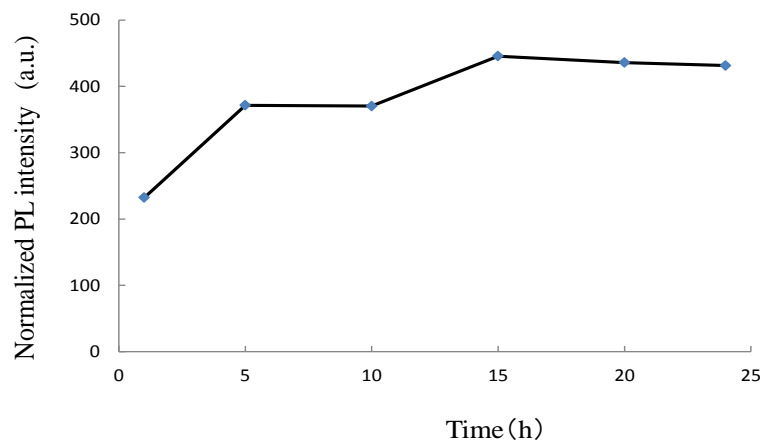
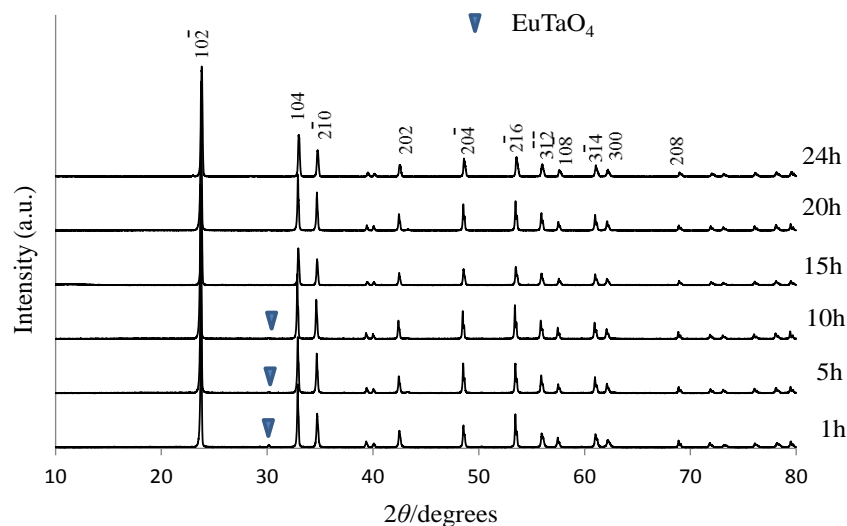


Figure 4. XRD patterns of $\text{Li}_{1.11}\text{Ta}_{0.89}\text{Ti}_{0.11}\text{O}_3:\text{Eu}^{3+}$ phosphors for various annealing times.



The LTT phosphors with various emission colors were synthesized while doping with trivalent ions of Sm, Er, Tm and Dy. The host material of $\text{Li}_{1.11}\text{Ta}_{0.89}\text{Ti}_{0.11}\text{O}_3$ was used at a fixed RE_2O_3 concentration of 2.5 wt %. Figure 5 shows the XRD patterns of LTT: RE^{3+} phosphors annealed for 15 h. All structures were LiTaO_3 -type, and no impurity phase was detected. The results show that the rare-earth ion diffused into the host material homogeneously and that rare-earth ions might also be located at the Li site. Emission peaks were compared between LNT: RE^{3+} and LTT: RE^{3+} phosphor, as shown in Figure 6. It should be mentioned here that the respective f-f excitations were much stronger than any possible charge-transfer excitations for the present LNT: RE^{3+} and LTT: RE^{3+} phosphors. The excitation wavelengths were then chosen with the strongest f-f excitations observed in each phosphor. Red emission of the Eu^{3+} -doped LTT was obviously brighter than that of LNT phosphor. Red emission was also observed for the Sm^{3+} -doped LNT upon excitation at around 411 nm due to the ${}^6\text{H}_{5/2}$ - ${}^6\text{P}_{3/2}$ transition. Upon excitation at 411 nm, the photoluminescence spectra showed emission peaks at 568 nm (${}^4\text{G}_{5/2}$ - ${}^6\text{H}_{5/2}$), 607 nm (${}^4\text{G}_{5/2}$ - ${}^6\text{H}_{7/2}$), and 651 nm (${}^4\text{G}_{5/2}$ - ${}^6\text{H}_{9/2}$). The splitting of the 607 nm emission is prominent in LNT phosphor. Therefore it seems that the peak intensity ratio of LTT phosphor at 607/651 nm is larger than that of LNT phosphor. This would be caused by the difference in the overlapping of orbitals with the adjacent anions (Ta/Nb). A green emission peak at 527 nm (${}^4\text{S}_{3/2}$ - ${}^4\text{I}_{15/2}$) was observed for LNT: Er^{3+} upon excitation at 552 nm (${}^4\text{I}_{15/2}$ - ${}^2\text{H}_{11/2}$). Blue emission was observed at 360 nm (${}^1\text{D}_2$ - ${}^3\text{F}_4$ transition) for the LNT: Tm^{3+} phosphor upon excitation at 463 nm (${}^3\text{H}_6$ - ${}^1\text{D}_2$). Yellow emission peaks at 584 nm (${}^4\text{F}_{9/2}$ - ${}^6\text{H}_{13/2}$) were observed for LNT: Dy^{3+} upon excitation at 355 nm (${}^6\text{H}_{15/2}$ - ${}^4\text{M}_{15/2}$). The highest emission peak intensity was compared between LNT: RE^{3+} and LTT: RE^{3+} . Green and Blue emissions of LNT phosphor were brighter than those of LTT phosphor. The internal quantum efficiency of these phosphors were low level; 23% for LTT: Sm^{3+} , 22% for LTT: Er^{3+} , 35% for LTT: Tm^{3+} , and 28% for LTT: Dy^{3+} .

Figure 5. XRD patterns of $\text{Li}_{1.11}\text{Ta}_{0.89}\text{Ti}_{0.11}\text{O}_3:\text{RE}^{3+}$ (RE: Dy, Tm, Er, Sm, Eu) for 15 h annealing.

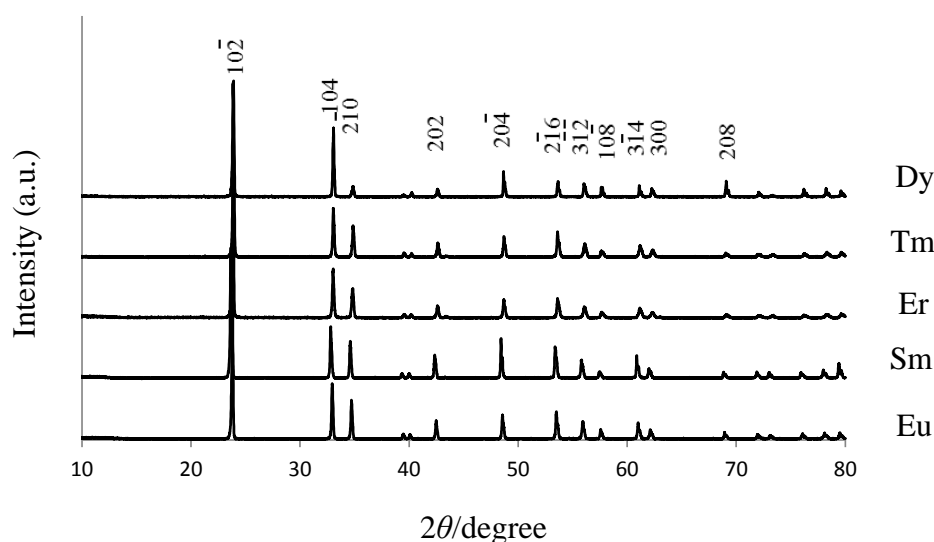
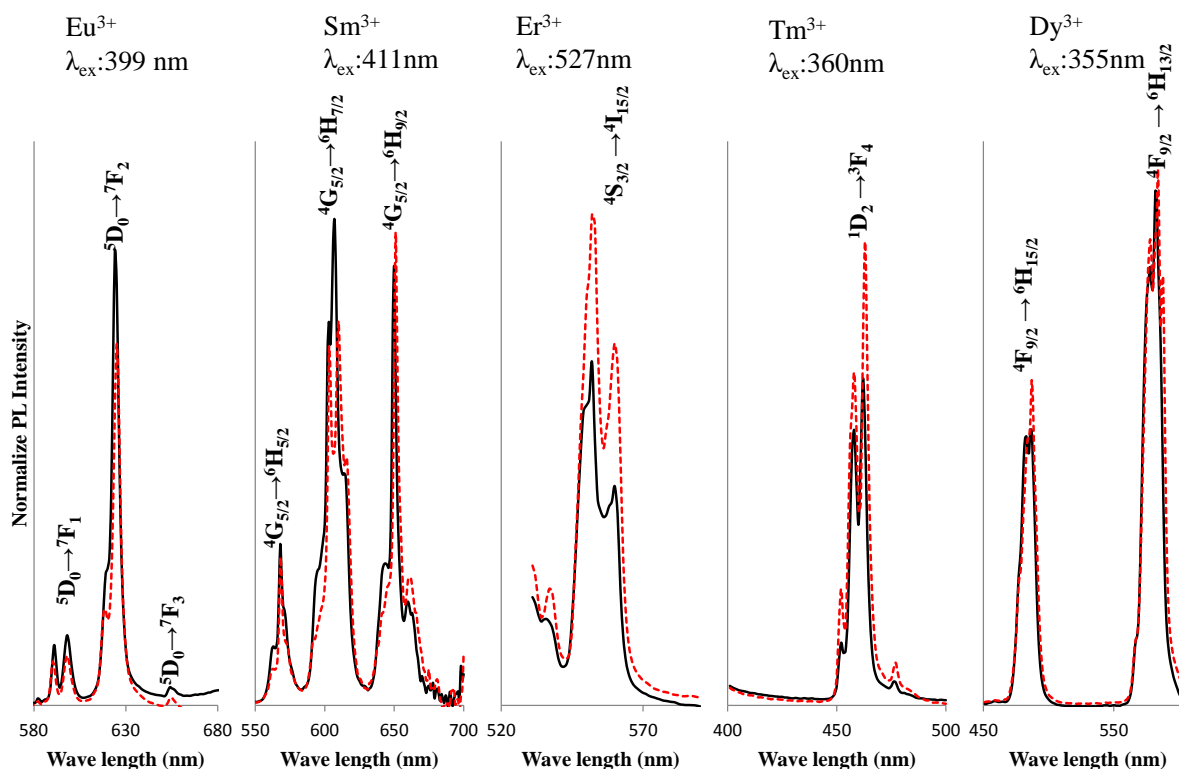


Figure 6. Comparison of PL intensity between LNT:RE³⁺ and LTT:RE³⁺. Dotted line: LNT:RE³⁺, solid line: LTT:RE³⁺.



In contrast, the most effective activator was the Eu³⁺ ion in the LTT host material. The red emission intensity excited at 339 nm of LTT: Eu³⁺ phosphor is three times higher than that of Y₂O₂S: Eu³⁺ (4.3 at %), which is well known as a red phosphor. It is assumed that small differences in the lattice site between LNT and LTT host materials would affect the transition probability of the respective RE³⁺ ions. The combination of the host material and the emitting RE³⁺ ion is of great significance in designing new phosphors. A more detailed structural analysis, and the relevant theoretical calculations, will be performed in the near future.

Table 1 shows the chromaticity (*x*, *y*) of the LNT:RE³⁺ and LTT:RE³⁺ phosphors in the red, green, blue and yellow color regions. In general, the PL behavior of the RE³⁺-doped phosphors is not affected by the host material's structure due to the 4f-4f transitions. In Sm phosphor, however, the difference in the emission intensity ratio at 606/650 nm affected the chromaticity.

Table 1. Chromaticity (*x*, *y*) of LNT and LTT phosphors.

Activator	LTT:RE ³⁺		LNT:RE ³⁺	
	<i>X</i>	<i>Y</i>	<i>X</i>	<i>Y</i>
Eu	0.673	0.327	0.676	0.324
Sm	0.622	0.378	0.630	0.370
Er	0.307	0.685	0.347	0.647
Tm	0.144	0.033	0.143	0.033
Dy	0.418	0.425	0.433	0.423

3. Experimental Procedure

The starting materials used were Li_2CO_3 , Ta_2O_5 and TiO_2 (>99.9% grade) to prepare the solid solution of LTT. The compositions of the LTT solid solutions prepared in this work followed the formula $\text{Li}_{1+x-y}\text{Ta}_{1-x-3y}\text{Ti}_{x+4y}\text{O}_3$ with $0.05 < x < 0.25$, $y = 0$ as a host material. Rare earths (Eu_2O_3 , Sm_2O_3 , Er_2O_3 , Tm_2O_3 and Dy_2O_3 > 99.9% grade) were doped in the host material. These powders were mixed and pressed in air at 1423 K for 1 h to 24h in a conventional electric furnace. As comparison materials, the rare earth doped $\text{Li}_{1+x}\text{Nb}_{1-x}\text{Ti}_x\text{O}_3$ (LNT) phosphors were also sintered at 1373 K for 24 h [13].

Structural analysis was carried out by X-ray diffraction (XRD) using a RINT 2500 (Rigaku Co., Ltd., Tokyo, Japan) operating at 40 kV and 200 mA. Microstructure images were observed by a scanning electron microscope (SEM) (SU8000, Hitachi Co., Ltd., Tokyo, Japan) operating at 3 kV. High-resolution TEM (HRTEM) images were observed by a device (2100 F, JEOL Co., Ltd., Tokyo, Japan) operating at 200 kV and equipped with energy-dispersed spectroscopy (EDS).

Excitation and emission spectra of the obtained samples were measured by a spectrometer (model FP-6500, JASCO international Co., Ltd., Tokyo, Japan). Quantum efficiency was measured by a spectral radiometer (MCPD-7000, Otsuka Electronics Co., Ltd., Osaka, Japan).

4. Conclusions

New phosphors have been successfully synthesized by doping rare-earth materials into a $\text{Li}_{1+x}\text{Ta}_{1-x}\text{Ti}_x\text{O}_3$ solid solution as a host material. The host material's structure and photoluminescence (PL) property was compared to the RE^{3+} -doped $\text{Li}_{1+x}\text{Nb}_{1-x}\text{Ti}_x\text{O}_3$ (LNT). The resulting materials showed various color emissions, with LNT:Eu³⁺ and LNT:Sm³⁺ exhibiting red emission, LNT:Tm³⁺ blue emission, LNT:Er³⁺ green emission, and LTT:Dy³⁺ yellow emission. The host material's structure of LTT phosphor with the optimal composition $\text{Li}_{1.11}\text{Nb}_{0.89}\text{Ti}_{0.11}\text{O}_3$ was not a superstructure. Therefore, the distortion due to superstructure did not affect the PL intensity in the LTT phosphor. The annealing time to synthesize the homogeneous phosphor was reduced from 24 h to 15 h. By doping Ti^{4+} and Eu^{3+} ions into the LiTaO_3 , the $\langle\text{Li-O}\rangle$ distance of the $[\text{LiO}_{12}]$ polyhedron in the LiTaO_3 structure (*R3c*) changed without a superstructure. This change affected the interaction with the adjacent anions, and the emission from the Eu^{3+} ion in the Li site achieved a high value of internal quantum efficiency. In the LTT host material, the most effective activator was the Eu^{3+} ion. On the other hand, the emission intensities of Er- and Tm-doped LTT phosphors were lower than that of LNT phosphor. We conclude that small differences in the lattice site between LNT and LTT host materials would affect the emission energy of the RE^{3+} ions.

Acknowledgments

We thank S. Yamada of Denki Kagaku Kogyo Co., Ltd. for help with our experiment. This work was partially supported by a research grant from The Murata Science Foundation (2012).

References

1. Villafuerte-Castrejon, M.E.; Gracia, J.A.; Cisneros, E.; Valenzuela, R.; West, A.R. New rutile solid solutions $Ti_{1-4x}Li_xM_{3x}O_2$; M = Nb, Ta, Sb. *J. Brit. Ceram. Soc.* **1984**, *83*, 143–145.
2. Villafuerte-Castrejon, M.E.; Aragon-Pina, A.; Valenzuela, R.; West, A.R. Compound and solid-solution formation in the system $Li_2O-Nb_2O_5-TiO_2$. *J. Solid State Ceram.* **1987**, *71*, 103–108.
3. Smith, R.I.; West, A.R. Characterization of an incommensurate LiTiNb oxide. *Mater. Res. Bull.* **1992**, *27*, 277–285.
4. Hayashi, H.; Nakano, H.; Suzumura, K.; Urabe, K.; West, A.R. Superstructure in LiTiNb oxides. *Forth Ceram. Soc.* **1995**, *2*, 391–398.
5. Hayashi, H.; Urabe, K.; Niihara, K. Preparation of stoichiometric crystalline $Li(Nb,Ti)O_3$ solid solutions by sol-gel processing with metal alkoxides. *Key Eng. Mater.* **1999**, *501*, 161–163.
6. Farber, L.; Levin, I.; Borisevichi, A.; Grey, I.E.; Roth, R.S.; Davies, P.K. Structural study of $Li_{1+x-y}Nb_{1-x-3y}Ti_{x+4y}O_3$ solid solutions. *J. Solid State Chem.* **2002**, *166*, 81–90.
7. Borisevich, A.Y.; Davies, P.K. Crystalline structure and dielectric properties of $Li_{1+x-y}Nb_{1-x-3y}Ti_{x+4y}O_3$ M-phase solid solutions. *J. Am. Ceram. Soc.* **2002**, *85*, 573–578.
8. Yamamoto, Y.; Hayashi, H.; Sekino, T.; Nakayama, T.; Kondo, T.; Wada, M.; Adachi, T.; Niihara, K. Microstructure and dielectric properties of sintered Li-Nb-Ti-O solid solution ceramics having superstructure. *Mater. Res. Innov.* **2003**, *7*, 74–79.
9. Hayashi, H.; Nakano, H. Evolution and preparation of $Li_{1+x-y}Nb_{1-x-3y}Ti_{x+4y}O_3$ solid solution with superstructure as new phosphor. *J. Alloy. Compd.* **2010**, *502*, 360–364.
10. Hayashi, H.; Nakano, H.; Jones, M.I. Microstructure and luminescence of Eu-doped $Li_{1+x-y}Nb_{1-x-3y}Ti_{x+4y}O_3$ solid solutions with superstructure. *J. Ceram. Soc. Jpn.* **2010**, *118*, 226–230.
11. Nakano, H.; Saji, T.; Yuasa, M.; Shoji, M.; Mamoru, M. Rapid synthesis and structural analysis of Li-Nb-Ti-O solid solutions with superstructure by millimeter-wave heating. *J. Ceram. Soc. Jpn.* **2011**, *119*, 808–812.
12. Nakano, H.; Ozono, K.; Saji, T.; Miyake, S.; Hiroyuki, H. Rapid synthesis of Eu^{3+} -doped LNT (Li-Nb-Ti-O) phosphor by millimeter-wave heating. *Opt. Mater.* **2012**, in press.
13. Nakano, H.; Suehrio, S.; Saji, T.; Miyake, S. Synthesis of a rare-earth doped LNT (Li-Nb-Ti-O) phosphor by millimeter-wave heating. *J. Alloy. Compd.* **2013**, 475–479.
14. Gryk, D.; Dyl, D.; Ryba-Romanowski, W.; Grinberg, M.; Spectral properties of $LiTaO_3:Pr^{3+}$ under high hydrostatic pressure. *J. Phys. Condens. Matter* **2005**, *17*, 5383–5395.
15. Kostritskii, S.M.; Maring, D.B.; Tavlykasev, R.F.; Ramaswamy, R.V. Energy transfer upconversion in Er-doped $LiTaO_3$. *Appl. Phys. Lett.* **2000**, *76*, 2161–2163.
16. Ryba-Romanowski, W.; Golab, S.; Dominiak-Dzik, G.; Paltnikov, M.N.; Sidorov, N.V. Influence of temperature on luminescence of terbium ions in $LiNbO_3$. *J. Appl. Lett.* **2001**, *78*, 3610–3611.
17. Gasparotto, G.; Cebin, M.A.; Goes, M.S.; Lima, S.A.M.; Davolos, M.R.; Varela, J.A.; Paiva-Santos, C.O.; Zaghete, M.A. Correlation between the spectroscopic and structural properties with the occupation of Eu^{3+} sites in powdered Eu^{3+} -doped $LiTaO_3$ prepared by the pechini method. *J. Appl. Phys.* **2009**, *106*, 3506–3509.

18. Sokolska, I.; Ryba-Romanowski, W.; Golab, S.; Baba, M.; Swirkowicz, M.; Lukasiewicz, T. Spectroscopy of $\text{LiTaO}_3:\text{Tm}^{3+}$ crystals. *J. Phys. Chem. Solids* **2000**, *61*, 1573–1581.
19. Nakano, H.; Ozono, K.; Hayashi, H.; Fujihara, S. Synthesis and luminescent properties of a new Eu^{3+} -doped $\text{Li}_{1+x}(\text{Ta}_{1-z}\text{Nb}_z)_{1-x}\text{Ti}_x\text{O}_3$ red phosphor. *J. Am. Ceram. Soc.* **2012**, 2795–2797.
20. Uchida, T.; Suehiro, S.; Asaka, T.; Nakano, H.; Fukuda, K. Syntheses and crystal structures of $\text{Li}(\text{Ta}_{0.89}\text{Ti}_{0.11})\text{O}_{2.945}$ and $(\text{Li}_{0.977}\text{Eu}_{0.023})(\text{Ta}_{0.89}\text{Ti}_{0.11})\text{O}_{2.968}$. *Powder Diffr.* **2013**, in press.

© 2013 by the authors; licensee MDPI, Basel, Switzerland. This article is an open access article distributed under the terms and conditions of the Creative Commons Attribution license (<http://creativecommons.org/licenses/by/3.0/>).